Harmonically confined *n*-electron systems coupled to light in a cavity: Time-dependent case

Chenhang Huang,[1] Cody Covington,[2] and Kálmán Varga[1,*]
[1]*Department of Physics and Astronomy, Vanderbilt University, Nashville, Tennessee 37235, USA*
[2]*Department of Chemistry, Austin Peay State University, Clarksville, Tennessee 37044, USA*

(Received 2 January 2023; revised 2 May 2023; accepted 31 May 2023; published 14 June 2023)

An analytically solvable time-dependent coupled light-matter problem is presented. An *n*-electron system is confined by a harmonic-oscillator potential and interacts with photons in a cavity. Both the electrons and the photons can interact with a time-dependent external field. The light-matter coupling is described by the Pauli-Fierz Hamiltonian. By separating the relative and center-of-mass motion, the Hamiltonian of the system can be simplified to a sum of a Hamiltonian of the relative and the center-of-mass motion. The Hamiltonian of the relative motion is time-independent, not coupled to light, and it can be solved by conventional approaches. The Hamiltonian of the center-of-mass motion reduces to that of a time-dependent harmonic oscillator and can be solved analytically. The analytical solution will be used to study excitations, the high-harmonic-generation spectrum, and nonlinear optical properties in a cavity.

DOI: 10.1103/PhysRevB.107.235130

I. INTRODUCTION

The interaction of light and matter in cavities is very successfully described by the Jaynes-Cummings (JC) model [1]. The predictions of the JC model have been experimentally tested [2–4], and new physical effects, e.g., Rabi oscillations [5], Fock states [6–8], squeezed states [9], entanglement of atoms and photons [10], Schrödinger cat states [11], and antibunching [12,13], are predicted.

The JC model was also extended to explicitly time-dependent Hamiltonians, e.g., a classical laser field is added to drive the system [14–20]. The coupling [21] or the frequency [22] can also be time-dependent. Time-dependent JC Hamiltonians where the driving field can couple either to the atom or to the cavity mode were also studied [23]. These approaches were used to model the dynamic Stark effect [23,24], synchronization of qubits [20], photon blockade [25], entanglement generation [24,26], highly excited Fock states [27], coherent states [28], induced atomic resonance fluorescence [29], or control of the quantum electromagnetic field [30] in cavities or superconducting circuits.

With the advance of experimental approaches, the study of systems with strong and ultrastrong light-matter coupling became the center of interest [31–42]. In the ultrastrong regime, the approximations of the JC model are not valid, and a new level of theoretical description is needed. The most popular and practical approach is based on the Pauli-Fierz (PF) Hamiltonian. The PF Hamiltonian describes the interaction between quantum matter (electrons) and a massless quantized radiation field (photons) in the low-energy nonrelativistic limit of quantum electrodynamics (QED) [43]. The PF approach has often been used in describing the modification of material properties in optical cavities [44–53]. In Ref. [54], we have shown that the PF Hamiltonian is analytically solvable for a harmonically confined two-electron system. Later, we extended the analytical solution to harmonically confined *n*-electron systems [55].

In this work, we will investigate a harmonically confined *n*-electron system in time-dependent driving fields. Two driving fields will be considered: an external laser pulse interacting with the electrons, and an external current interacting with the photons. As the electrons and the photons are coupled, the external field acting on the electrons excites the photons and vice versa. Coupled electrons and photons in external fields haven been studied using perturbation theory [56,57] or with numerical approaches [58]. The effect of light-matter coupling on electron-electron interaction and correlation in laser-driven cavities has been investigated [59–62].

The wave function of the harmonically confined electron systems can be factorized into a relative motion and a center-of-mass motion part. The wave function of the relative motion is time-independent and it can be solved analytically for $N = 2$ electrons [54] or numerically for $N > 2$ electrons [55]. The center-of-mass Hamiltonian is coupled to light and it is time-dependent. This Hamiltonian can be separated into a sum of laser-driven time-dependent one-dimensional harmonic-oscillator Hamiltonians. These Hamiltonians have analytic solutions, or alternatively they can be solved by exact diagonalization and time-propagation, as will be shown in this paper.

Numerical calculations will be presented to show how the time-dependent external fields can be used to excite photons and electrons. We will show that by a suitable chosen external field, the system can be excited to a desired photon number state. One-photon states have been experimentally generated for quantum computer applications using entangled atoms [7,8]. Our calculations show that states with a fixed number of photons can also be created using quantum dots with harmonic confinement. The external fields can also change the high-harmonic-generation (HHG) spectra and the nonlinear properties of the system. The tunability of

*kalman.varga@vanderbilt.edu

the nonlinear properties of molecules has been studied in Ref. [63] using the QED time-dependent density functional theory [58,64,65]. In this work, we study these effects in an analytically solvable model system. The numerical examples highlight several interesting possibilities. In the case of HHG, the coupling to the cavity can remove inversion symmetry and even harmonics can appear in the spectrum. The coupling also introduces new polaritonic excitation peaks that appear in the HHG spectrum. The position of these peaks is independent of the frequency of the exciting laser field, but it depends on the confining potential and the cavity parameters. Thus, the HHG spectrum can be altered by the cavity and it is not only determined by the driving field. It will also be shown that the nonlinear susceptibility can be tuned by the coupling strength and the cavity frequency. We have found that the susceptibility strongly depends on the occupation of the excited states. The occupation of the excited states can be tuned by the cavity frequency and the light-matter coupling. The occupation increases with stronger coupling, but it has a maximum value as a function of the frequency. The nonlinear susceptibilities follow a similar tendency.

The outline of the paper is as follows. In Sec. II the formalism is introduced, and the separation of the Hamiltonian into exactly solvable terms is presented. In Sec. III the diagonalization of the coupled light center-of mass Hamiltonian is discussed. In Sec. IV numerical calculations for the laser-driven Hamiltonian are considered. This is followed by a short summary. Appendixes are included to make the paper self-contained.

II. FORMALISM

We assume that the system is nonrelativistic and the coupling to the light can be described by the dipole approximation (the wavelength of light is much larger than the size of the system). The nonrelativistic PF QED Hamiltonian provides a consistent quantum description at this level. The PF Hamiltonian in the Coulomb gauge [44–48] is

$$H = H_e + H_{ep}, \tag{1}$$

$$H_e = \sum_{i=1}^{N}\left(-\frac{\hbar^2}{2m_e}\vec{\nabla}_i^2 + v_{\text{ext}}(\mathbf{r}_i,t)\right) + \frac{e^2}{4\pi\epsilon_0}\sum_{i>j}^{N}\frac{1}{|\mathbf{r}_i-\mathbf{r}_j|},$$

$$H_{ep} = \sum_{\alpha=1}^{N_p}\left\{\frac{1}{2}\left[\hat{p}_\alpha^2 + \omega_\alpha^2\left(\hat{q}_\alpha - \frac{\boldsymbol{\lambda}_\alpha}{\omega_\alpha}\cdot\mathbf{D}\right)^2\right] + \frac{j_{\text{ext}}^{(\alpha)}(t)}{\omega_\alpha}\hat{q}_\alpha\right\}, \tag{2}$$

where $\mathbf{r}_i$ are the positions, m_e is the mass, and e is the charge of the electrons. In Eq. (2) the photon fields are described by quantized oscillators using raising and lowering operators $\hat{a}_\alpha$ and $\hat{a}_\alpha^+$. $\mathbf{D}$ is the dipole operator,

$$\mathbf{D} = \sum_{i=1}^{N}\mathbf{r}_i, \tag{3}$$

where N is the number of electrons and

$$q_\alpha = \sqrt{\frac{\hbar}{2\omega_\alpha}}(\hat{a}_\alpha^+ + \hat{a}_\alpha) \tag{4}$$

is the displacement field. p_α is the canonical conjugate momentum to q_α, which can be written as

$$p_\alpha = i\sqrt{\frac{\hbar\omega_\alpha}{2}}(\hat{a}_\alpha^+ - \hat{a}_\alpha). \tag{5}$$

In addition to the static terms, a time-dependent external potential, $v_{\text{ext}}(\mathbf{r}_i,t)$, interacts with the electrons, and a time-dependent external current, $j_{\text{ext}}^{(\alpha)}(t)$, interacts with the photons. The Hamiltonian in Eq. (2) describes N_p photon modes with photon frequency ω_α and coupling $\boldsymbol{\lambda}_\alpha$. The coupling term is usually written as [66] $\boldsymbol{\lambda}_\alpha = \sqrt{4\pi}\,S_\alpha(\mathbf{r})\mathbf{e}_\alpha$, where $S_\alpha(\mathbf{r})$ is the cavity mode function at position $\mathbf{r}$, and $\mathbf{e}_\alpha$ is the transversal polarization vector of the photon modes.

The external potential will be taken in the form

$$\begin{aligned} v_{\text{ext}}(\mathbf{r}_i,t) &= \frac{1}{2}m_e^2\omega_0^2\sum_{i=1}^{N}\mathbf{r}_i^2 + \mathbf{E}_{\text{ext}}(t)\mathbf{D} \\ &= \frac{1}{2}m_e^2\frac{\omega_0^2}{N}\left[\sum_{i<j}^{N}(\mathbf{r}_i-\mathbf{r}_j)^2 + \left(\sum_{i=1}^{N}\mathbf{r}_i\right)^2\right] \\ &\quad + \mathbf{E}_{\text{ext}}(t)\mathbf{D}, \end{aligned} \tag{6}$$

which is a sum of harmonic-oscillator confinements and an external electric pulse described as a classical field. In the second line, we have used an identity that will be useful later in this section.

Atomic units are used; $\hbar$, e, m_e, and $4\pi\epsilon_0$ are all equal to unity and may be dropped from the equations.

One can define $N-1$ relative coordinates (see Appendix A for more details)

$$\mathbf{x}_i = \mathbf{r}_i - \mathbf{R}\ \ (i=1,\ldots,N-1), \quad \mathbf{R} = \frac{1}{N}\sum_{j=1}^{N}\mathbf{r}_j. \tag{7}$$

Many different relative coordinate systems can be defined (two are presented, and the relation between them is discussed in Appendix A). The above choice is particularly simple because the single-particle coordinates can be expressed as

$$\mathbf{r}_i = \mathbf{x}_i + \mathbf{R}\ \ (i=1,\ldots,N-1), \quad \mathbf{r}_N = -\sum_{j=1}^{N-1}\mathbf{x}_j + \mathbf{R}. \tag{8}$$

The Hamiltonian for the electrons can be written as

$$H_e = H_{\mathbf{x}} + H_{\mathbf{R}}, \tag{9}$$

with

$$H_{\mathbf{x}} = \frac{1}{2}\sum_{i=1}^{N-1}\boldsymbol{\pi}_i^2 + \frac{1}{2}\frac{\omega_0^2}{N}\sum_{i<j}^{N}(\mathbf{r}_i-\mathbf{r}_j)^2 + \frac{1}{2}\sum_{i<j}^{N}\frac{1}{|\mathbf{r}_i-\mathbf{r}_j|} \tag{10}$$

and

$$H_{\mathbf{R}} = \frac{1}{2N}\mathbf{P}^2 + \frac{1}{2}N\omega_0^2\mathbf{R}^2 + N\mathbf{E}_{\text{ext}}(t)\mathbf{R}, \tag{11}$$

where $\mathbf{P}$ is the canonically conjugate momentum to $\mathbf{R}$, and $\boldsymbol{\pi}_i$ are canonically conjugate momenta to $\mathbf{x}_i$. Note that $H_{\mathbf{x}}$ depends on $\mathbf{r}_i-\mathbf{r}_j$, but using Eq. (8), $\mathbf{r}_i-\mathbf{r}_j$ can be expressed using the $N-1$ relative coordinates $\mathbf{x}_k$ and there is no dependence on $\mathbf{R}$.

Assuming that we have only one photon mode with frequency ω and defining the coupling term as $\boldsymbol{\lambda} = \lambda(1, 1, 0)$, the electron-photon coupling term becomes

$$H_{ep} = \omega\left(\hat{a}^+\hat{a} + \frac{1}{2}\right) - N\omega\hat{q}\boldsymbol{\lambda}\mathbf{R} + \frac{1}{2}N^2(\boldsymbol{\lambda}\mathbf{R})^2 + \frac{j_{\text{ext}}(t)}{\omega}\hat{q}. \tag{12}$$

The generalization to many-photon modes and different forms of $\boldsymbol{\lambda}$ is simple and can be found in Ref. [55]. To simplify the notation and make the paper more readable, we will restrict to a single mode and the above-defined $\boldsymbol{\lambda}$.

Now the total Hamiltonian can be written as

$$H = H_{\mathbf{x}} + \left[\omega\left(\hat{a}^+\hat{a} + \frac{1}{2}\right) + \frac{j_{\text{ext}}(t)}{\omega}\hat{q}\right] - N\omega q\boldsymbol{\lambda}\mathbf{R} + \left(H_{\mathbf{R}} + \frac{1}{2}N^2(\boldsymbol{\lambda}\mathbf{R})^2\right). \tag{13}$$

The first term is the Hamiltonian of the relative motion. It is not coupled to the center-of-mass motion or to the photon space, and it is time-independent. For $N = 2$ electrons, $H_{\mathbf{x}}$ can be solved analytically [54]; for more than two electrons, it can be treated numerically [55].

The terms in the square brackets represent the Hamiltonian of the photons coupled to the center-of-mass through the third term ($N\omega q\boldsymbol{\lambda}\mathbf{R}$). The terms in the large parentheses represent the Hamiltonian acting on the center-of-mass motion.

As is shown in Appendix B, the Hamiltonian can be decoupled into the following form:

$$H = H_{\mathbf{x}} + H_v + H_z + H_c, \tag{14}$$

where

$$H_c = \omega\left(\hat{a}^+\hat{a} + \frac{1}{2}\right) - \omega q\sqrt{2N}\lambda u + \frac{j_{\text{ext}}(t)}{\omega}\hat{q} + H_u. \tag{15}$$

Here H_u, H_v, and H_z are one-dimensional time-dependent harmonic-oscillator functions. These are analytically solvable [67,68] (see Appendix C), and the time-dependent eigenfunctions $\phi_v(v, t)$ and $\phi_z(z, t)$ are known. We note that as is discussed in Appendix B, one can simplify the model further by assuming an external field defined as $\mathbf{E}_{\text{ext}}(t) = (E(t), E(t), 0)$. In that case, ϕ_v and ϕ_z are time-independent harmonic-oscillator functions.

The ansatz

$$\Psi = \Phi(\mathbf{x})e^{-iE_{\mathbf{x}}t}\phi_v(v, t)\phi_z(z, t)\Phi_c(u, t) \tag{16}$$

satisfies the time-dependent Schrödinger equation

$$i\frac{\partial}{\partial t}\Psi = H\Psi. \tag{17}$$

The wave functions Φ_x, ϕ_v, and ϕ_z are already known, and we only need to deal with H_c, as will be discussed in the next section.

III. DIAGONALIZATION OF THE LIGHT-MATTER COUPLED HAMILTONIAN

The Hamiltonian H_c can be diagonalized in two different ways. In the first approach, new variables are introduced to decouple the CM and photon harmonic oscillators. In the second one, a product basis of the CM and photon harmonic oscillators $\phi_k(u)|n\rangle$ is used, where $\phi_k(u)$ satisfies the time-independent equation

$$H_u\phi_k(u) = \left(k + \tfrac{1}{2}\right)\omega_u\phi_k(u), \quad \omega_u^2 = \omega_0^2 + 2N\lambda^2 \tag{18}$$

(see Appendix B). The advantage of the first approach is that it is exact, while numerical diagonalization is needed in the second approach. The advantage of the second approach is that the solution is directly obtained as a product of spatial and photon spaces.

A. Shifted Fock states

The coupling Hamiltonian can be rewritten as

$$H_c = -\frac{1}{2}\frac{\partial^2}{\partial q^2} + \frac{1}{2}\omega^2 q^2 - \frac{1}{2}\frac{\partial^2}{\partial u^2} + \frac{1}{2}\omega_u^2 u^2 + \kappa uq + \epsilon_q q + \epsilon_u u, \tag{19}$$

with

$$\kappa = -\omega\sqrt{2N}\lambda, \quad \epsilon_q = \frac{j_{\text{ext}}(t)}{\omega}. \tag{20}$$

This is a Hamiltonian of two coupled time-dependent harmonic oscillators. The Hamiltonian can be decoupled by introducing the following coordinate rotations:

$$r = q\cos\theta - u\sin\theta, \quad s = q\sin\theta + u\cos\theta, \tag{21}$$

with $\tan 2\theta = \frac{2\kappa}{\omega_u^2 - \omega^2}$. The Hamiltonian is decoupled into two uncoupled time-dependent harmonic oscillators

$$H_c = H_r + H_s, \tag{22}$$

$$H_r = -\frac{1}{2}\frac{\partial^2}{\partial r^2} + \frac{1}{2}\omega_r^2 r^2 + c_r(t)r,$$
$$H_s = -\frac{1}{2}\frac{\partial^2}{\partial s^2} + \frac{1}{2}\omega_s^2 s^2 + c_s(t)s, \tag{23}$$

where

$$\omega_r^2 = \omega^2\cos^2\theta + \omega_u^2\sin^2\theta - \kappa\sin 2\theta,$$
$$\omega_s^2 = \omega^2\sin^2\theta + \omega_u^2\cos^2\theta + \kappa\sin 2\theta, \tag{24}$$

and

$$c_r(t) = \epsilon_q\cos\theta - \epsilon_u\sin\theta,$$
$$c_s(t) = \epsilon_q\sin\theta + \epsilon_u\cos\theta. \tag{25}$$

Now the analytical solution can be written as a product of the eigenfunctions of H_r and H_s in Eq. (23) as outlined in Appendix C.

B. Exact diagonalization

The Hamiltonian in Eq. (15) can also be solved by exact diagonalization using the product of center-of-mass eigenfunctions and photon Fock states as basis states,

$$|n_u, n_q\rangle = \phi_{n_u}(u)|n_q\rangle. \tag{26}$$

To diagonalize H_c, one needs the matrix elements of the Hamiltonian which are readily available. The operators H_u and u act on the real space, and $\hat{a} + \hat{a}^+$ acts on the photon space.

The matrix elements of q and u are

$$\langle m|q|n\rangle = \frac{1}{\sqrt{2\omega}} D_{mn}, \tag{27}$$

$$\langle i|u|j\rangle = \frac{1}{\sqrt{2\omega_u}} D_{ij}, \tag{28}$$

where

$$D_{mn} = \begin{pmatrix} 0 & \sqrt{1} & 0 & 0 & 0 & \cdots \\ \sqrt{1} & 0 & \sqrt{2} & 0 & 0 & \cdots \\ 0 & \sqrt{2} & 0 & \sqrt{3} & 0 & \cdots \\ 0 & 0 & \sqrt{3} & 0 & \sqrt{4} & \cdots \\ 0 & 0 & 0 & \sqrt{4} & 0 & \cdots \\ \vdots & \vdots & \vdots & \vdots & \vdots & \ddots \end{pmatrix}. \tag{29}$$

Thus, the matrix elements of H_c are

$$\begin{aligned} \langle i, m|H_c|j, n\rangle = {} & \delta_{mn}\delta_{ij}\left(j + \frac{1}{2}\right)\omega_u + \delta_{mn}\delta_{ij}\left(n + \frac{1}{2}\right)\omega \\ & + \frac{k}{2\sqrt{\omega\omega_u}} D_{mn} D_{ij} + \frac{\epsilon_u(t)}{\sqrt{2\omega_u}} D_{ij}\delta_{nm} \\ & + \frac{\epsilon_q(t)}{\sqrt{2\omega}} D_{nm}\delta_{ij}. \end{aligned} \tag{30}$$

After the diagonalization, we have the eigenenergies and the eigenfunctions. The eigenfunction has the following form:

$$\Phi_c = \sum_{n_u, n_q} c_{n_u, n_q} \phi_{n_u}(u)|n_q\rangle, \tag{31}$$

where c_{n_u,n_q} are the components of the eigenvector.

In the large-N limit, we have $\omega_u \approx \sqrt{2N}\lambda$, and the coupling strength in the last term of Eq. (30) will be

$$\sqrt{\omega}(N/8)^{1/4}, \tag{32}$$

which is independent of λ. In this case, ω_u is very large, and the lowest u harmonic-oscillator state dominates,

$$\Phi_c = \sum_{n_q} c_{0,n_q} \phi_0(u)|n_q\rangle. \tag{33}$$

IV. RESULTS

In this section, we present numerical examples using the exact diagonalization approach. The advantage of this method is that the matter and photon coordinates are factorized, and one can analyze the weight of the matter and light components in the wave function easily.

First one has to construct a product basis

$$\phi_{n_u}(u)|n_q\rangle, \tag{34}$$

where the highest n_u and n_q values depend on the coupling strength, on the frequency of light, and on the confining harmonic-oscillator potential. One can easily find the appropriate values by testing the convergence of the lowest energies as a function of the basis dimension.

The converged ground or excited state,

$$\Phi_c(t = 0) = \sum_{n_u, n_q} c_{n_u, n_q} \phi_{n_u}(u)|n_q\rangle, \tag{35}$$

will be time-propagated to solve the time-dependent problem. In the time propagation, the basis is time-independent but the linear coefficients change in time, and the wave function is

$$\Phi_c(t) = \sum_{n_u, n_q} c_{n_u, n_q}(t) \phi_{n_u}(u)|n_q\rangle. \tag{36}$$

We will use the Crank-Nicolson [69] time-propagator to solve the time-dependent Schrödinger-equation:

$$\Phi_c(t + \Delta t) = \exp\left(-\frac{i}{\hbar} H \Delta t\right) \Phi_c(t) \tag{37}$$

$$\approx \frac{1 - \frac{i}{2} H \Delta t}{1 + \frac{i}{2} H \Delta t} \Phi_c(t), \tag{38}$$

where H is the Hamiltonian matrix defined in Eq. (30). The Crank-Nicolson method is unconditionally stable, and with an appropriately small time step, it converges to the exact solution [70]. In our case, the dimension of H is low so the calculation of the inverse in the Crank-Nicolson step is computationally cheap, but H is very sparse and one could use iterative inversion even for H of large dimensions. Atomic units will be used in the calculations.

We will calculate the following quantities:

(i) Norm of the wave function as a function of time,

$$|\Phi_c(t)|^2 = \sum_{n_u, n_q} \left|c_{n_u, n_q}(t)\right|^2. \tag{39}$$

This is a good measure of the accuracy of the time propagation. The norm remains 1 if the time step is suitably chosen, and it will diverge if the time step is too large.

(ii) The occupation probability of a given CM harmonic-oscillator wave function as a function of time,

$$\Phi_{\rm cm}(n_u, t) = \sum_{n_q} \left|c_{n_u, n_q}(t)\right|^2. \tag{40}$$

This function shows how the oscillator states are excited during the external time-dependent pulse.

(iii) The occupation probability of a given photon state as a function of time,

$$\Phi_{\rm ph}(n_q, t) = \sum_{n_u} \left|c_{n_u, n_q}(t)\right|^2. \tag{41}$$

This shows the excitation of the photon states.

(iv) The time-dependent expectation value of the Hamiltonian,

$$\begin{aligned} E &= \langle \Phi_c(t)|H_c|\Phi_c(t)\rangle \\ &= \sum_{n_u, n_q} \sum_{n'_u, n'_q} c_{n_u, n_q}(t)^* c_{n'_u, n'_q}(t) \langle n_u, n_q|H_c|n'_u, n'_q\rangle. \end{aligned} \tag{42}$$

Note that this quantity is not constant because the energy of the electromagnetic field is not added. This quantity shows the change of the energy of a time-propagated state compared to the initial state.

(v) The time-dependent dipole moment for the center-of-mass,

$$u(t) = \langle \Phi_c(t)|u|\Phi_c(t)\rangle = \frac{1}{\sqrt{2\omega_u}} \sum_{n_u,n_u',n_q} c_{n_u,n_q}(t)^* c_{n_u',n_q}(t) D_{n_u n_u'}, \quad (43)$$

where $D_{nn'}$ is defined in Eq. (29).

(vi) The high harmonic spectrum is calculated using the dipole acceleration,

$$I(\omega_h) = \left| \int_0^T \frac{\partial^2 u(t)}{\partial t^2} e^{-i\omega_h t} dt \right|^2. \quad (44)$$

To calculate the high harmonic spectrum, we time-propagate a system in a laser pulse, calculate $u(t)$, and then $I(\omega)$.

(vii) The nonlinear susceptibilities. Using an electric field $E_i f(t)$ that is sufficiently weak, the induced dipole moment $u_i(t)$ can be expressed in power series [71,72],

$$u_i(t) = \sum_n p^{(n)}(t)(E_i)^n, \quad (45)$$

where $p^{(n)}(t)$ is the nth-order component of the polarization. The polarization, $p^{(n)}$, can be expressed using the nth-order susceptibility $\chi^{(n)}$ as

$$p^{(n)}(t) = \int \chi^{(n)}(t-t_1, t-t_2, \ldots, t-t_n) \times f(t_1) f(t_2) \cdots f(t_n) dt_1 dt_2 \cdots dt_n, \quad (46)$$

and this describes the nonlinear optical properties of the system. To calculate $\chi^{(n)}$, one time-propagates the system subject to $E_i f(t)$ for several values of E_i and inverts Eq. (45) to get $p^{(n)}(t)$. Then $\chi^{(n)}$ can be extracted from (46) [71,72].

A. Excitation by an external field

In this case, the system is subject to a time-dependent external field of the form

$$\epsilon_q(t) = E_e f(t), \quad f(t) = g\left(\frac{20\pi}{\omega_e}, \frac{32\pi}{\omega_e}, t\right) \sin(\omega_e t), \quad (47)$$

where E_e is the strength of the excitation, ω_e is the excitation frequency, and the envelope function is defined as a trapezoidal,

$$g(a,b,t) = \begin{cases} \frac{2t}{b-a}, & t < \frac{1}{2}(b-a), \\ 1, & \frac{1}{2}(b-a) \leqslant t < \frac{1}{2}(a+b), \\ 1 - 2\frac{t-\frac{a+b}{2}}{(b-a)}, & t > \frac{1}{2}(a+b), \\ 0, & t > b. \end{cases} \quad (48)$$

As Eq. (19) shows, the coupling Hamiltonian is symmetric in ϵ_q and ϵ_u. The former excites the photons through the coupling to the photon displacement q, and the latter excites the electrons through coupling to the dipole moment.

Figure 1 shows the excitation caused by the external field. We will investigate the cavity frequency and the coupling strength dependence of the wave functions using the first excited state. The ground state only shows oscillation following the oscillation of the external excitation, but the order of states does not change for physically realistic parameter sets. In

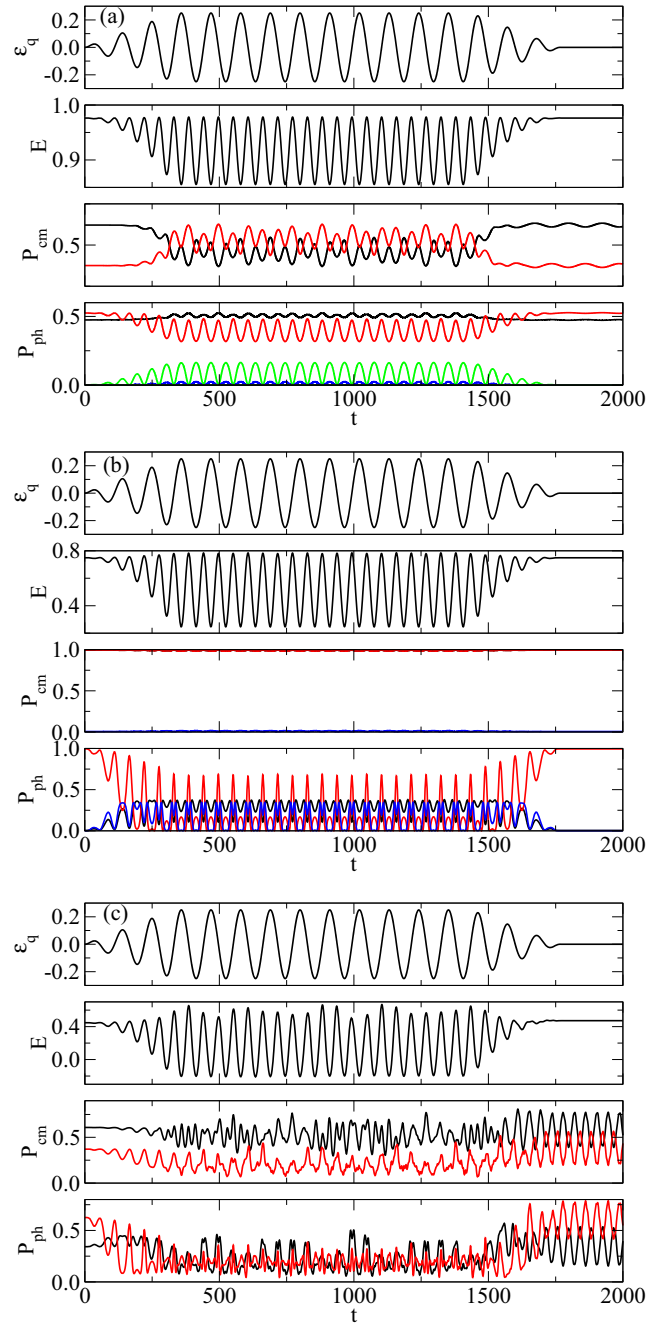

FIG. 1. Time propagation of the light-matter coupled system. (a) External pulse, energy, center-of-mass, and photon number occupation probability as a function of time for $N = 2$ electrons with $\omega_0 = 0.5$, $\omega = 0.5$, and $\lambda = 0.025$. The starting state is the first excited state, $\Phi_c = 0.69\phi_1(u)|0\rangle + 0.72\phi_0(u)|1\rangle$. (b) External pulse, energy, center-of-mass, and photon number occupation probability as a function of time for $N = 2$ electrons with $\omega_0 = 0.5$, $\omega = 0.25$, and $\lambda = 0.025$. The starting state is the first excited state, $\Phi_c = \phi_0(u)|1\rangle$. (c) External pulse, energy, center-of-mass, and photon number occupation probability as a function of time for $N = 2$ electrons with $\omega_0 = 0.25$, $\omega = 0.25$, and $\lambda = 0.075$. The starting state is the first excited state, $\Phi_c = 0.58\phi_1(u)|0\rangle + 0.78\phi_0(u)|1\rangle + 0.13\phi_2(u)|1\rangle$. $\omega_e = 0.057$ is used in the calculations. In the occupation number figures, the black curve corresponds to quantum number 0, the red to 1, the green to 2, and the blue to 3. The green and blue are not shown in (c) because they would overlap the other curves.

the case of the first excited state, there are changes in level order depending on the parameters of the cavity. By appropriate choice of parameters, one can drive the system into a desired photon number state as experimentally described in Refs. [7,8].

In Fig. 1(a), the first excited state and an entangled state of the photon states $|0\rangle$ and $|1\rangle$ are time-propagated. The oscillation of the energy and occupation numbers follows the oscillation of the laser field. The highest occupied CM harmonic-oscillator occupation state oscillates between the $n_u = 0$ and 1 states. The order of the higher occupied photon states changes at the beginning and the end of the laser pulse. The occupation of the $|2\rangle$ photon states also increases significantly.

In the second case [Fig. 1(b)], λ is kept the same but ω is decreased. As Eq. (30) shows, this decreases the coupling between the CM motion and photons but increases the strength of the external field. As a consequence, the starting first-excited state is almost purely a $\Phi_c = \phi_0(u)|1\rangle$ state and the occupations of the harmonic-oscillator states barely change. The occupations of the photon states and the order of the states, however, change rapidly.

In the third case, we increase λ. In this case, the coupling is stronger and the starting wave function $[\Phi_c = 0.58\phi_1(u)|0\rangle + 0.78\phi_0(u)|1\rangle + 0.13\phi_2(u)|1\rangle]$ contains higher harmonic-oscillator components. The oscillation of the energy and occupation numbers become irregular because the higher harmonic oscillator and photon states get excited. Moreover, the oscillations of the occupation numbers continue after the laser pulse in a Rabi-oscillation-like manner. These examples show that changing the coupling, cavity frequency, and harmonic confinement can generate a variety of coupled light-matter states with an external field.

B. High harmonic generation

Figure 2 shows the high harmonic spectrum of the system calculated using Eq. (44). The system is subject to a Gaussian envelope laser pulse

$$\epsilon_u(t) = E_e f(t), \quad f(t) = \exp\left(-\frac{(t-\tau)^2}{\sigma^2}\right)\sin(\omega_e t), \quad (49)$$

and time propagated for 100 000 time units. Note that in this case, the CM motion dipole is excited by ϵ_u [see Eq. (30)]. Figure 2(a) shows the HHG for the noncoupled, $\lambda = 0$, $\omega = 0$ case. Due to the inversion symmetry of the CM harmonic-oscillator Hamiltonian, only the odd harmonics appear in the spectrum at $n\omega_e$ for $n = 1, 3, 5, \ldots$. Once the light and matter degrees of freedom are coupled [Figs. 2(b), 2(c), and 2(d)], the inversion symmetry is lost and even harmonics can appear depending on the coupling and the cavity frequency.

Figure 2 shows (blue arrows) the position of the excitation energies of the lowest eigenstates of the time-dependent Hamiltonian [defined by the first three terms in Eq. (30)]. If the coupling is weak, then the first two terms of Eq. (30) determine the eigenenergies. The dipole operator couples states $\phi_i|n\rangle$ and $\phi_j|m\rangle$ if $n = m$ and $j = i \pm 1$ [see Eq. (30)].

In the case of no coupling, the lowest states are $\phi_0|0\rangle$, $\phi_1|0\rangle$, $\phi_2|0\rangle$ and the excitation energies shown in Fig. 2(a) are ω_u and $2\omega_u$ (the excitation energy is defined by subtracting the ground-state energy from the energy of the given state). One can see that a peak appears at the position of the excitation energies corresponding to the transitions from the ground state to the excited states due to the laser.

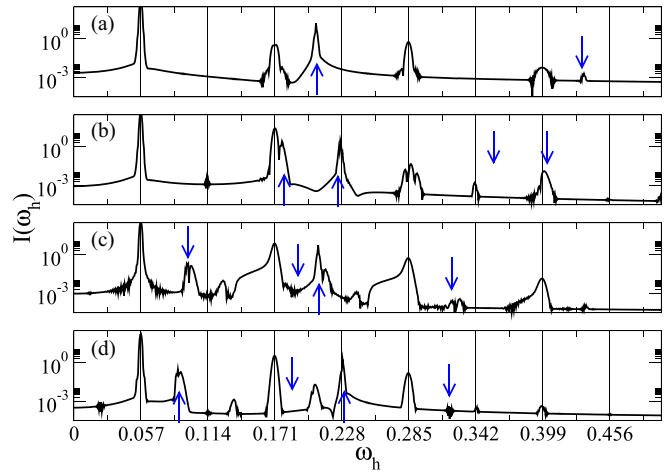

FIG. 2. High harmonic spectra. (a) No coupling; (b) $\omega = 0.2$, $\lambda = 0.025$; (c) $\omega = 0.1$, $\lambda = 0.025$; (d) $\omega = 0.1$, $\lambda = 0.05$. The exciting laser is defined by Eq. (49) with $E_e = 0.2$, $\omega_e = 0.057$, $\tau = 5067$ $\sigma = 2067$, and $T = 100\,000$. The red and blue bars show the positions of the excitation energy of the lowest states of the time-independent system. The excitation energy is defined as the difference between the energy of the excited state minus the energy of the ground state.

The same trend can be observed for the $\omega > 0$ and $\lambda > 0$ cases [see, e.g., Fig. 2(b)] but now the spectrum is more complex due to the coupling to light. The lowest states are

$$\begin{aligned}
\Phi_{c0} &\approx 0.99\phi_0|0\rangle + 0.06\phi_1|1\rangle,\\
\Phi_{c1} &\approx 0.66\phi_1|0\rangle - 0.74\phi_0|1\rangle,\\
\Phi_{c2} &\approx 0.74\phi_1|0\rangle + 0.66\phi_0|1\rangle,\\
\Phi_{c3} &\approx 0.05\phi_0|0\rangle - 0.46\phi_2|0\rangle + 0.71\phi_1|1\rangle,\\
\Phi_{c4} &\approx -0.69\phi_2|0\rangle + 0.08\phi_1|1\rangle + 0.71\phi_0|2\rangle. \quad (50)
\end{aligned}$$

The transition from Φ_{c0} to Φ_{c1} and Φ_{c2} is strong because Φ_{c1} and Φ_{c2} have large $\phi_1|0\rangle$ components. These two transition peaks are visible, although the first partly overlaps with the peaks at the laser frequency. The excitation energies corresponding to Φ_{c3} and Φ_{c4} do not appear in the spectrum because the wave-function components are much smaller. Transitions from and to other states are also possible but less significant. The excitation energy peaks in Figs. 2(c) and 2(d) can be explained similarly. Compared to Figs. 2(b), 2(c) is calculated for a smaller cavity frequency. The main effect is that the excitation energies are different and the corresponding peaks are shifted. A similar effect can be observed in Fig. 2(d), but in this case the peaks are moved by increasing λ.

This example shows that the HHG of the system changed in the cavity due to two main effects. The first is that the coupling removed the inversion symmetry restriction, allowing the possible appearance of even harmonics. Secondly, the energy levels of the harmonically confined electrons in the cavity show up in the HHG spectrum. As the energy levels

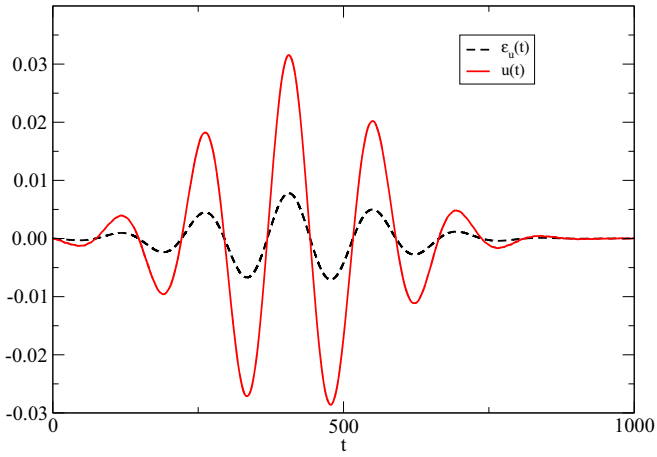

FIG. 3. Polarization and electric field. The laser is defined by Eq. (49) with parameters $\omega_e = 0.043$, $\tau = 413$, and $\sigma = 206$. Laser strength $E_e = 0.0078$ was used to calculate $u(t)$.

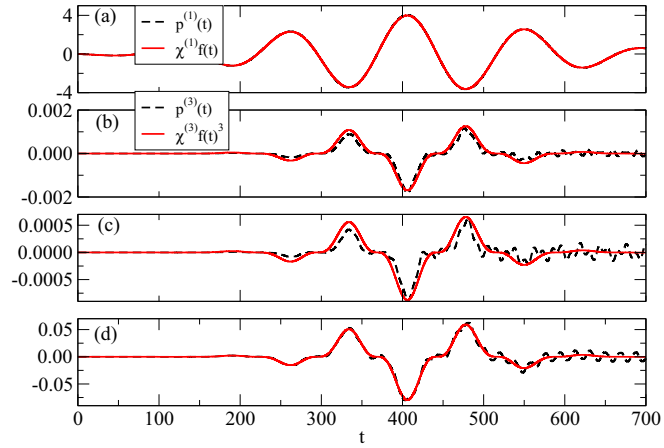

FIG. 4. First- and third-order susceptibilities. (a) $p^{(1)}(t)$ (dashed black) and $\chi^{(1)}f(t)$ (red) ($\chi^{(1)} = 4$). (b) $p^{(3)}(t)$ (dashed black) and $\chi^{(3)}f(t)^3$ (red) ($\chi^{(3)} = 0.0017$) for $\omega_0 = 0.5$, $\omega = 0.5$, and $\lambda = 0.1$. (c) $p^{(3)}(t)$ (dashed black) and $\chi^{(3)}f(t)^3$ (red) ($\chi^{(3)} = 0.000\,88$) for $\omega_0 = 0.5$, $\omega = 0.25$, and $\lambda = 0.1$. (d) $p^{(3)}(t)$ (dashed black) and $\chi^{(3)}f(t)^3$ (red) ($\chi^{(3)} = 0.008$) for $\omega_0 = 0.5$, $\omega = 0.5$, and $\lambda = 0.2$. The legend of (b) is also a legend of (c) and (d). The laser is defined by Eq. (49) with parameters $\omega_e = 0.043$, $\tau = 413$, and $\sigma = 206$. Three laser strengths, $E_{ei} = 0.001\,95, 0.0039, 0.0078$, were used to calculate $p^{(n)}$.

depend on ω_0, ω, and λ, one can add HHG peaks at desired positions and can modulate the HHG spectrum with the cavity.

C. Nonlinear susceptibilities

In this section, we calculate the nonlinear susceptibilities for certain cavity parameters. The nonlinear susceptibilities of molecules in cavities have been studied in Ref. [63]. It was found that the polaritonic resonances can enhance the susceptibilities, and the nonlinear conversion efficiency can be tuned by the coupling strength.

Using Eq. (46) we have calculated the polarizations up to the third order. The exciting electric field is typically a few-cycle laser pulse, and the pulse used in this calculation [Eq. (49)] is similar to the choice of Refs. [71,72]. The frequency of the confining harmonic-oscillator potential is chosen to be $\omega_0 = 0.5$. The cavity frequency ω and the coupling λ are selected in such a way that the occupation of the excited state is small. In these cases, the susceptibilities can be extracted using a simple fit. If the excited states are more dominant, then the calculation of the frequency-dependent susceptibilities will be more tedious.

Figure 3 shows the external field and the polarization for a weak laser field. The time-dependent dipole moment smoothly follows the oscillation of the laser. By calculating the dipole moments $u_i(t)$ for three different laser field strengths, E_{ei} [see Eq. (49)], we can calculate $p^{(n)}$ using Eq. (45). The values of $p^{(n)}$ are not sensitive to the values of E_{ei} provided that the field is sufficiently weak. Figure 4 shows that $p^{(n)}$ can be very well approximated by $\chi^{(n)}f(t)^n$, which is a simple time- (or frequency-) independent susceptibility. Figure 4(a) shows that the linear component, $\chi^{(1)} = 4$, gives an excellent fit to $p^{(1)}(t)$. Figures 4(b), 4(c), and 4(d) show the dependence of $p^{(3)}$ on ω and λ. These figures show that a simple $p^{(3)} = \chi^{(3)}f(t)^3$ gives a good fit for the third-order polarization, although the fit is not as perfect as for the first-order one. Note that while the calculation of the time-dependent dipole is very accurate, the extraction of $\chi^{(1)}$ has to be averaged over time, which introduces an error bar of about $\pm 5\%$ due to the fluctuation of the polarization.

Figure 5 shows the dependence of second- and third-order susceptibility on λ and ω. The calculations show that the dependence of χ on ω and λ is closely related to the occupation probability. The value of $\chi^{(n)}$ increases when the occupation of excited states is higher because more states will be connected with dipole transitions. We have investigated the dependence of the occupation probability on the cavity frequency and coupling in Ref. [55], and now we apply those finding for this case. Figure 5(a) shows the occupation of the excited states as a function of ω. For a fixed λ, two terms in Eq. (30) influence the occupation of the excited states. By increasing ω, the second term shifts the energy of the excited states higher, and that decreases the occupation probability of the excited states. The third term couples the center-of-mass and the photon spaces, and the coupling is proportional to $\sqrt{\omega}$. By increasing ω, the coupling increases, and that leads to higher excited-state occupation probability. As a result of these two competing processes, the occupation of the excited states first increases with ω and then reaches a maximum and starts to decrease, as is shown in Fig. 5(a). The behavior of $\chi^{(n)}$ is very similar [Fig. 5(b)], increasing and reaching a maximum before starting to decrease. The curve is not as smooth as the occupation probability due to the error related to the extraction. A similar behavior can be found for the λ dependence of the occupation number and $\chi^{(2)}$ [see Figs. 5(c) and 5(d)]. In this case, the occupation number increases monotonically with λ because λ is larger than the coupling [third term in Eq. (30)]. The second-order polarization $\chi^{(2)}$ is much smaller than the third-order one. The small value of $\chi^{(2)}$ is due to the fact that the second-order process is not allowed without coupling to the cavity, and it remains hindered for the parameter region of this study.

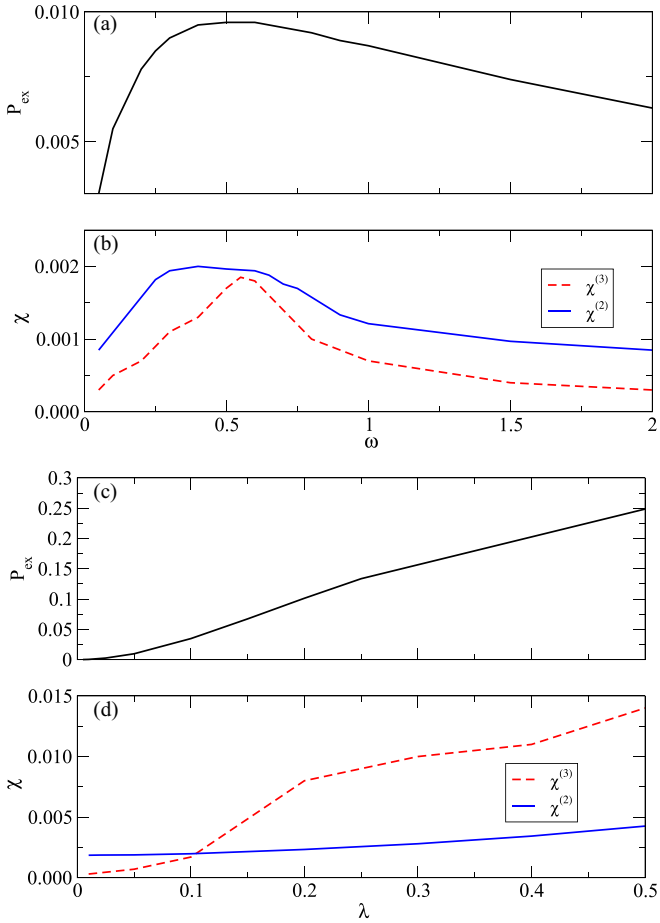

FIG. 5. Dependence of occupation probability of the excited states and the nonlinear susceptibilities $\chi^{(n)}$ on the cavity frequency and the coupling strength. $\chi^{(2)}$ is multiplied by 800 to fit in the same figure as $\chi^{(2)}$. $\lambda = 0.1$ and $\omega_0 = 0.5$ are used for the ω dependence, and $\omega = 0.5$ and $\omega_0 = 0.5$ are used for the λ dependence.

V. SUMMARY

We have presented an analytically solvable time-dependent model of the interaction of harmonically confined electrons and light in a cavity. In the framework of the Pauli-Fierz Hamiltonian, the relative motion and center-of-mass motion can be factorized. The Hamiltonian of the relative motion is time-independent and it is not coupled to light. It can be solved by various approaches as we have described in Refs. [54,55]. The Hamiltonian of the center-of-mass motion can be written as the sum of three Hamiltonians, each of them depending on a single variable only. This separation allows the factorization of the center-of-mass wave function into a product form so that the three Hamiltonians can be solved independently. Two of these Hamiltonians are not coupled to the light, and these are simple time-dependent harmonic-oscillator Hamiltonians that can be solved analytically (see Appendix C). The third Hamiltonian is a coupled light-matter harmonic-oscillator Hamiltonian. This Hamiltonian can be decoupled by using shifted Fock states, and it can be solved analytically.

The disadvantage of the analytical solution is that in the wave functions, the light and matter coordinates are mixed and it is cumbersome to calculate physical properties in terms of light or matter degrees only. As an alternative, we use a product of harmonic oscillators and Fock states as a basis that allows an exact diagonalization approach. The convergence can be controlled by increasing the number of orthogonal basis states. This product basis can also be used to solve the time-dependent problem with time propagation of the wave function.

Three different time-dependent problems are studied. In the first, we have shown how external fields acting on either the light or the matter degrees of freedom can excite the other degrees of freedom. In the second, the effect of the cavity on the HHG spectrum was investigated. We have shown that with the cavity, one can introduce intensity peaks in the HHG spectrum at desired locations which may have applications in ultrafast (attosecond) spectroscopies. In the third example, we have shown how the third-order nonlinear susceptibility (which is an important quantity controlling nonlinear optical mixing processes) of the system changes and can be tuned in the cavity.

ACKNOWLEDGMENTS

This work has been supported by the National Science Foundation (NSF) under Grant No. 2217759.

APPENDIX A: RELATIVE COORDINATES

In a system of N particles with coordinates $\mathbf{r}_i$, one can introduce $N-1$ independent relative coordinates $\mathbf{x}_i$ and a center-of-mass coordinate $\mathbf{R} = \mathbf{x}_N$ by a linear transformation [73]

$$\mathbf{x}_i = \sum_{j=1}^{N} U_{ij}\mathbf{r}_j. \tag{A1}$$

Many different choices of definitions of the relative coordinate set are used, for example

$$U = \begin{pmatrix} 1 & -1 & 0 & 0 & \cdots & 0 \\ \frac{1}{2} & \frac{1}{2} & -1 & 0 & \cdots & 0 \\ \vdots & \vdots & \vdots & \ddots & \vdots & 0 \\ \frac{1}{N-1} & \frac{1}{N-1} & \frac{1}{N-1} & \frac{1}{N-1} & \vdots & -1 \\ \frac{1}{N} & \frac{1}{N} & \frac{1}{N} & \frac{1}{N} & \frac{1}{N} & \frac{1}{N} \end{pmatrix}$$

or

$$U' = \begin{pmatrix} 1-\frac{1}{N} & -\frac{1}{N} & -\frac{1}{N} & \cdots & -\frac{1}{N} \\ -\frac{1}{N} & 1-\frac{1}{N} & -\frac{1}{N} & \cdots & -\frac{1}{N} \\ \vdots & \vdots & \ddots & \vdots & \vdots \\ -\frac{1}{N} & -\frac{1}{N} & \vdots & 1-\frac{1}{N} & -\frac{1}{N} \\ \frac{1}{N} & \frac{1}{N} & \frac{1}{N} & \frac{1}{N} & \frac{1}{N} \end{pmatrix},$$

and the generalization for unequal masses is straightforward [73]. The U matrices can be inverted and the different relative coordinates can be transformed into each other. The inverse of

the transformation matrices is

$$U^{-1} = \begin{pmatrix} \frac{1}{2} & \frac{1}{3} & \frac{1}{4} & \cdots & \frac{1}{N-1} & 1 \\ -\frac{1}{2} & \frac{1}{3} & \frac{1}{4} & \cdots & \frac{1}{N-1} & 1 \\ 0 & -\frac{1}{3} & \frac{1}{4} & \cdots & \frac{1}{N-1} & 1 \\ \vdots & \vdots & \vdots & \ddots & \vdots & \vdots \\ 0 & 0 & 0 & \cdots & -\frac{N-1}{N} & 1 \end{pmatrix},$$

and

$$U'^{-1} = \begin{pmatrix} 1 & 0 & 0 & \cdots & 0 & 1 \\ 0 & 1 & 0 & \cdots & 0 & 1 \\ 0 & 0 & 1 & \cdots & 0 & 1 \\ \vdots & \vdots & \vdots & \ddots & \vdots & \vdots \\ -1 & -1 & -1 & \cdots & -1 & 1 \end{pmatrix}.$$

As all elements of the last row of U are $1/N$, the inverse matrix has a special structure: all elements of its last column are 1 [73]. That means that we can express the single-particle coordinates as

$$\mathbf{r}_i = \sum_{j=1}^{N-1} U^{-1}_{ij} \mathbf{x}_j + \mathbf{R}. \tag{A2}$$

The relative and center-of-mass momenta $\boldsymbol{\pi}_i = -i\hbar \frac{\partial}{\partial \mathbf{x}_i}$ are related to the single-particle momenta $\mathbf{p}_i = -i\hbar \frac{\partial}{\partial \mathbf{r}_i}$ as

$$\boldsymbol{\pi}_i = \sum_{j=1}^{N} U^{-1}_{ji} \mathbf{p}_j \;\; (i = 1, \ldots, N). \tag{A3}$$

This equation defines the total momentum as $\boldsymbol{\pi}_i = \sum_{j=1}^{N} \mathbf{p}_j$, and the center-of-mass kinetic energy is $T_{\rm cm} = \boldsymbol{\pi}_N^2/2N$. Now we can subtract the center-of-mass kinetic energy from the total kinetic energy

$$\sum_{i=1}^{N} \frac{\mathbf{p}_i^2}{2} - T_{\rm cm} = \frac{1}{2} \sum_{i=1}^{N-1} \sum_{j=1}^{N-1} \Lambda_{ij} \boldsymbol{\pi}_i \boldsymbol{\pi}_j, \tag{A4}$$

where

$$\Lambda_{ij} = \sum_{k=1}^{N} U_{ik} U_{jk}. \tag{A5}$$

This completes the separation of the relative and center-of-mass system, and it works in any system defined by U.

As an example, let us consider $N = 3$. Using U, one can define

$$\begin{aligned} \mathbf{x}_1 &= \mathbf{r}_1 - \mathbf{r}_2, \\ \mathbf{x}_2 &= \frac{\mathbf{r}_1 + \mathbf{r}_2}{2} - \mathbf{r}_3, \\ \mathbf{R} &= \frac{\mathbf{r}_1 + \mathbf{r}_2 + \mathbf{r}_3}{3}, \end{aligned} \tag{A6}$$

and the single-particle coordinates are expressed as

$$\begin{aligned} \mathbf{r}_1 &= \tfrac{1}{2}\mathbf{x}_1 + \tfrac{1}{3}\mathbf{x}_2 + \mathbf{R}, \\ \mathbf{r}_2 &= -\tfrac{1}{2}\mathbf{x}_1 + \tfrac{1}{3}\mathbf{x}_2 + \mathbf{R}, \\ \mathbf{r}_3 &= -\tfrac{2}{3}\mathbf{x}_2 + \mathbf{R}. \end{aligned} \tag{A7}$$

Similarly, using U' we can define

$$\begin{aligned} \mathbf{x}'_1 &= \frac{2}{3}\mathbf{r}_1 - \frac{1}{3}\mathbf{r}_2 - \frac{1}{3}\mathbf{r}_3, \\ \mathbf{x}'_2 &= -\frac{1}{3}\mathbf{r}_1 + \frac{2}{3}\mathbf{r}_2 - \frac{1}{3}\mathbf{r}_3, \\ \mathbf{R} &= \frac{\mathbf{r}_1 + \mathbf{r}_2 + \mathbf{r}_3}{3}, \end{aligned} \tag{A8}$$

and now the single-particle coordinates are

$$\begin{aligned} \mathbf{r}_1 &= \mathbf{x}'_1 + \mathbf{R}, \quad \mathbf{r}_2 = \mathbf{x}'_2 + \mathbf{R}, \\ \mathbf{r}_3 &= -\mathbf{x}'_1 - \mathbf{x}'_2 + \mathbf{R}. \end{aligned} \tag{A9}$$

APPENDIX B: DECOUPLING THE CENTER-OF-MASS HAMILTONIAN

The center-of-mass part can be simplified further by introducing

$$u = \sqrt{N}\frac{X+Y}{\sqrt{2}}, \quad v = \sqrt{N}\frac{Y-X}{\sqrt{2}}, \quad z = \sqrt{N}Z, \tag{B1}$$

where $\mathbf{R} = (X, Y, Z)$, and

$$\epsilon_u(t) = \sqrt{N}\frac{E_x(t) + E_y(t)}{\sqrt{2}}, \tag{B2}$$

$$\begin{aligned} \epsilon_v(t) &= \sqrt{N}\frac{E_x(t) - E_y(t)}{\sqrt{2}}, \\ \epsilon_z(t) &= \sqrt{N}E_z(t), \end{aligned} \tag{B3}$$

where $\mathbf{E}_{\rm ext}(t) = (E_x(t), E_y(t), E_z(t))$. Using this notation, the light-matter coupling term becomes

$$\omega q \boldsymbol{\lambda} \mathbf{R} = \omega q \sqrt{2N} \lambda u, \tag{B4}$$

and only the u coordinate is coupled to light. By defining

$$H_u = -\frac{1}{2}\frac{\partial^2}{\partial u^2} + \frac{1}{2}\omega_u^2 u^2 + \epsilon_u(t) u, \tag{B5}$$

$$\begin{aligned} H_v &= -\frac{1}{2}\frac{\partial^2}{\partial v^2} + \frac{1}{2}\omega_v^2 v^2 + \epsilon_v(t) v, \\ H_z &= -\frac{1}{2}\frac{\partial^2}{\partial z^2} + \frac{1}{2}\omega_z^2 z^2 + \epsilon_z(t) z, \end{aligned} \tag{B6}$$

with frequencies

$$\omega_u^2 = \omega_0^2 + 2N\lambda^2, \quad \omega_v^2 = \omega_z^2 = \omega_0^2, \tag{B7}$$

we can write the CM part as

$$H_{\mathbf{R}} + \tfrac{1}{2}N^2(\boldsymbol{\lambda}\mathbf{R})^2 = H_u + H_v + H_z. \tag{B8}$$

Now the CM Hamiltonian is a sum of three independent time-dependent harmonic oscillators, and only H_u is coupled with light. This derivation can be easily generalized to any form of $\boldsymbol{\lambda}$ [54], and it is not limited to the present $\boldsymbol{\lambda} = \lambda(1, 1, 0)$ choice as we have mentioned before. These time-dependent Hamiltonians have known analytical solutions [67,68], which have been reviewed in Appendix C. If one chooses $E_x = E_y$ and $E_z = 0$, then H_v and H_z are time-independent and the solution is even simpler.

Now we can define a simplified coupling Hamiltonian in the following form:

$$H_c = \omega\left(\hat{a}^+\hat{a} + \frac{1}{2}\right) - \omega q\sqrt{2N}\lambda u + \frac{j_{\text{ext}}(t)}{\omega}\hat{q} + H_u. \quad \text{(B9)}$$

The total Hamiltonian now becomes

$$H = H_{\mathbf{x}} + H_v + H_z + H_c. \quad \text{(B10)}$$

By solving the Schrödinger equation for the time-independent part,

$$H_{\mathbf{x}}\Phi(\mathbf{x}) = E_{\mathbf{x}}\Phi(\mathbf{x}), \quad \text{(B11)}$$

and solving the time-dependent Schrödinger equations for the time-dependent parts,

$$i\frac{\partial}{\partial t}\phi_v(v,t) = H_v\phi_v(v,t), \quad \text{(B12)}$$

$$i\frac{\partial}{\partial t}\phi_z(z,t) = H_z\phi_z(z,t), \quad \text{(B13)}$$

$$i\frac{\partial}{\partial t}\Phi_c(u,t) = H_c\Phi_c(u,t). \quad \text{(B14)}$$

The ansatz

$$\Psi = \Phi(\mathbf{x})\mathrm{e}^{-iE_{\mathbf{x}}t}\phi_v(v,t)\phi_z(z,t)\Phi_c(u,t) \quad \text{(B15)}$$

satisfies the time-dependent Schrödinger equation

$$i\frac{\partial}{\partial t}\Psi = H\Psi. \quad \text{(B16)}$$

APPENDIX C: SOLUTION OF THE TIME-DEPENDENT HARMONIC-OSCILLATOR HAMILTONIAN

The time-dependent Schrödinger equation for a harmonic oscillator driven by a laser field is analytically solvable [67,68]. We include the key ingredients in this Appendix for completeness. The starting equation is

$$-\frac{\hbar^2}{2m}\frac{\partial^2}{\partial x^2} + \left[\frac{1}{2}kx^2 - xF(t)\right]\psi = i\hbar\frac{\partial\psi}{\partial t}, \quad \text{(C1)}$$

where $F(t)$ is a time-dependent driving field.

Rewrite ψ into the form

$$\psi(x,t) = \chi(x,t)e^{g(t)x}, \quad \chi(x,t) = \phi(x-u(t),t), \quad \text{(C2)}$$

where $u(t)$ and $g(t)$ are auxiliary functions to be determined. By substituting this ansatz into Eq. (C1), one has

$$-\frac{\hbar^2}{2m}\frac{\partial^2\phi}{\partial\xi^2} + \left(i\hbar\dot{u} - \frac{\hbar^2}{m}g\right)\frac{\partial\phi}{\partial\xi} + \frac{1}{2}k\xi^2\phi + (ku - F - i\hbar\dot{g})\xi\phi + \left(\frac{1}{2}ku^2 - Fu - i\hbar u\dot{g} - \frac{\hbar^2}{2m}g^2\right)\phi = i\hbar\frac{\partial\phi}{\partial t}, \quad \text{(C3)}$$

where $\xi = x - u(t)$. Now we can choose g and u to eliminate the coefficients of $\partial\phi/\partial\xi$ and $\xi\phi$,

$$i\hbar\dot{u} - \frac{\hbar^2}{m}g = 0, \quad ku - F - i\hbar\dot{g} = 0 \quad \text{(C4)}$$

and Eq. (C3) simplifies to

$$-\frac{\hbar^2}{2m}\frac{\partial^2\phi}{\partial\xi^2} + \frac{1}{2}k\xi^2\phi = i\hbar\frac{\partial\phi}{\partial t} - \delta(t)\phi, \quad \text{(C5)}$$

where we have defined

$$\delta(t) = \frac{1}{2}ku^2 - Fu - i\hbar u\dot{g} - \frac{\hbar^2}{2m}g^2 = \frac{1}{2}m\dot{u}^2 - \frac{1}{2}ku^2, \quad \text{(C6)}$$

where the second equality is obtained by using Eqs. (C4).

In Eq. (C5), the ξ and t variables are separable, and the left-hand side represents the time-independent harmonic oscillators, with eigenenergies $E_n = (n + \frac{1}{2})\hbar\omega$ and wave functions

$$N_n \exp\left(-\tfrac{1}{2}\alpha^2\xi^2\right)H_n(\alpha\xi), \quad \text{(C7)}$$

where H_n is the nth Hermite polynomial,

$$\alpha^4 = mk/\hbar^2, \quad \omega = [k/m]^{\frac{1}{2}}, \quad \text{(C8)}$$

$$N_{n^2} = \frac{\alpha}{\pi^{\frac{1}{2}}2^n n!}. \quad \text{(C9)}$$

The right-hand side can be integrated over time, and the total solution is

$$\phi = N_n \exp\left\{-\frac{i}{\hbar}\int[\delta(t) + E_n]dt\right\}\exp\left(-\frac{1}{2}\alpha^2\xi^2\right)H_n(\alpha\xi). \quad \text{(C10)}$$

Note that Eq. (C4) is equivalent to a driven classical harmonic-oscillator equation

$$m\ddot{u} + ku = F(t), \quad \text{(C11)}$$

and g is also uniquely determined by solving for u in this equation.

As a simple example, we consider a sinusoidal driving field of the electrons: $\epsilon_q = 0$, $\epsilon_u = C_F\cos(\omega_F t)$ in (18). The transformed driving fields $c_r(t)$, $c_s(t)$, corresponding to $F(t)$ above, are still of the form $C_F\cos(\omega_F t)$. The solution to (C11) is well known,

$$u = A_1\exp(i\omega t) + A_2\exp(-i\omega t) + \frac{C_F}{|\omega^2 - \omega_F^2|}\cos(\omega_F t), \quad \text{(C12)}$$

where A_1, A_2 are given by the initial conditions, and ω is the oscillator frequency. Note that the complex parts of u should not be dropped, as they affect the time-dependency of the wave functions. One can easily evaluate the integral:

$$\int\delta(t)dt = \frac{i\omega}{2}\left(A_1^2e^{2i\omega t} - A_2^2e^{-2i\omega t}\right) - \frac{C_F^2 t}{4\left(\omega^2 - \omega_F^2\right)} - \frac{C_F^2\left(\omega^2 + \omega_F^2\right)}{8\omega_F\left(\omega^2 - \omega_F^2\right)^2}\sin(2\omega_F t) + \frac{i\omega C_F\left(A_1e^{i\omega t} - A_2e^{-i\omega t}\right)}{|\omega^2 - \omega_F^2|}\cos(\omega_F t). \quad \text{(C13)}$$

Thus, the time-dependent wave function is determined.

In our case, the analytical solution for H_c [Eq. (23)] can be written as a product of the eigenfunctions of H_r and H_s,

$$\Phi_c = \chi_r\chi_s\phi_{r,n}\phi_{s,m}, \quad \text{(C14)}$$

where

$$\phi_{r,n} = N_{r,n} \exp\left\{-i\int[\delta_r(t)+E_n]\,dt - \frac{1}{2}\omega_r\xi_r^2\right\} H_n(\sqrt{\omega_r}\xi_r), \tag{C15}$$

$$N_{r,n} = \left(\frac{\omega_r}{\pi}\right)^{\frac{1}{4}} \frac{1}{\sqrt{2^n n!}},\ E_n = \left(n+\frac{1}{2}\right)\omega_r, \tag{C16}$$

$$\delta_r(t) = \frac{1}{2}\dot{w}^2 - \frac{1}{2}\omega_r^2 w^2,\ \xi_r(t) = r - w(t),$$

$$\chi_r = \exp(ir\dot{w}). \tag{C17}$$

H_n is the nth Hermite polynomials, and $w(t)$ is the solution to $\ddot{w} + \omega_r^2 w = -c_r(t)$, which has exact particular solutions in integral form for any reasonable $c_r(t)$. Appendix C shows an analytical example. The χ_s and $\phi_{s,m}$ are obtained analogously. In principle, any starting wave function can be decomposed through a basis formed by $\phi_{r,n}$ at $t = 0$ and time-propagated by evolving each $\phi_{r,n}$.

APPENDIX D: DECOUPLING

Suppose the following Hamiltonian:

$$H = -\frac{1}{2}\frac{\partial^2}{\partial x^2} - \frac{1}{2}\frac{\partial^2}{\partial y^2} + \frac{1}{2}\omega_x^2 x^2 + \frac{1}{2}\omega_y^2 y^2 + kxy + a(t)x + b(t)y. \tag{D1}$$

Assume the following transformations:

$$u = x\cos\theta - y\sin\theta,\quad v = x\sin\theta + y\cos\theta. \tag{D2}$$

Then we decouple the Hamiltonian

$$H = H_u + H_v, \tag{D3}$$

where

$$H_u = -\frac{1}{2}\frac{\partial^2}{\partial u^2} + \frac{1}{2}\omega_u^2 u^2 + c(t)u,$$

$$H_v = -\frac{1}{2}\frac{\partial^2}{\partial v^2} + \frac{1}{2}\omega_v^2 v^2 + d(t)v, \tag{D4}$$

and

$$c = a\cos\theta - b\sin\theta,\ d = a\sin\theta + b\cos\theta. \tag{D5}$$

The rotational angle is given by

$$\tan 2\theta = -\frac{2k}{\omega_x^2 - \omega_y^2} \tag{D6}$$

and the frequencies

$$\omega_u^2 = \omega_x^2\cos^2\theta + \omega_y^2\sin^2\theta - k\sin 2\theta, \tag{D7}$$

$$\omega_v^2 = \omega_x^2\sin^2\theta + \omega_y^2\cos^2\theta + k\sin 2\theta. \tag{D8}$$

H_u and H_v can be solved by Appendix C.

[1] E. Jaynes and F. Cummings, Comparison of quantum and semiclassical radiation theories with application to the beam maser, Proc. IEEE **51**, 89 (1963).

[2] S. Haroche and J. Raimond, *Radiative Properties of Rydberg States in Resonant Cavities*, edited by D. Bates and B. Bederson (Academic Press, 1985), pp. 347–411.

[3] D. Meschede, H. Walther, and G. Müller, One-Atom Maser, Phys. Rev. Lett. **54**, 551 (1985).

[4] G. Rempe, H. Walther, and N. Klein, Observation of Quantum Collapse and Revival in a One-atom Maser, Phys. Rev. Lett. **58**, 353 (1987).

[5] I. I. Rabi, On the process of space quantization, Phys. Rev. **49**, 324 (1936).

[6] J. J. Slosser, P. Meystre, and S. L. Braunstein, Harmonic Oscillator Driven by a Quantum Current, Phys. Rev. Lett. **63**, 934 (1989).

[7] S. Brattke, B. T. H. Varcoe, and H. Walther, Generation of Photon Number States on Demand via Cavity Quantum Electrodynamics, Phys. Rev. Lett. **86**, 3534 (2001).

[8] M. Weidinger, B. T. H. Varcoe, R. Heerlein, and H. Walther, Trapping States in the Micromaser, Phys. Rev. Lett. **82**, 3795 (1999).

[9] M. Hillery, Squeezing and photon number in the Jaynes-Cummings model, Phys. Rev. A **39**, 1556 (1989).

[10] S. Bose, I. Fuentes-Guridi, P. L. Knight, and V. Vedral, Subsystem Purity as an Enforcer of Entanglement, Phys. Rev. Lett. **87**, 050401 (2001).

[11] M. Brune, S. Haroche, J. M. Raimond, L. Davidovich, and N. Zagury, Manipulation of photons in a cavity by dispersive atom-field coupling: Quantum-nondemolition measurements and generation of "schrödinger cat" states, Phys. Rev. A **45**, 5193 (1992).

[12] F. Dubin, D. Rotter, M. Mukherjee, C. Russo, J. Eschner, and R. Blatt, Photon Correlation versus Interference of Single-Atom Fluorescence in a Half-Cavity, Phys. Rev. Lett. **98**, 183003 (2007).

[13] M. Hennrich, A. Kuhn, and G. Rempe, Transition from Antibunching to Bunching in Cavity QED, Phys. Rev. Lett. **94**, 053604 (2005).

[14] F. Krumm and W. Vogel, Time-dependent nonlinear Jaynes-Cummings dynamics of a trapped ion, Phys. Rev. A **97**, 043806 (2018).

[15] A. Joshi, Nonlinear dynamical evolution of the driven two-photon Jaynes-Cummings model, Phys. Rev. A **62**, 043812 (2000).

[16] M. S. Abdalla, E. Khalil, and A.-F. Obada, Exact treatment of the Jaynes–Cummings model under the action of an external classical field, Ann. Phys. **326**, 2486 (2011).

[17] F.-l. Li and S.-y. Gao, Controlling nonclassical properties of the Jaynes-Cummings model by an external coherent field, Phys. Rev. A **62**, 043809 (2000).

[18] C. A. Blockley, D. F. Walls, and H. Risken, Quantum collapses and revivals in a quantized trap, Europhys. Lett. **17**, 509 (1992).

[19] L. Ermann, G. G. Carlo, A. D. Chepelianskii, and D. L. Shepelyansky, Jaynes-Cummings model under monochromatic driving, Phys. Rev. A **102**, 033729 (2020).

[20] O. V. Zhirov and D. L. Shepelyansky, Synchronization and Bistability of a Qubit Coupled to a Driven Dissipative Oscillator, Phys. Rev. Lett. **100**, 014101 (2008).

[21] A. Joshi and S. V. Lawande, Generalized Jaynes-Cummings models with a time-dependent atom-field coupling, Phys. Rev. A **48**, 2276 (1993).
[22] Y. Yang, J. Xu, G. Li, and H. Chen, Interactions of a two-level atom and a field with a time-varying frequency, Phys. Rev. A **69**, 053406 (2004).
[23] P. Alsing, D.-S. Guo, and H. J. Carmichael, Dynamic stark effect for the Jaynes-Cummings system, Phys. Rev. A **45**, 5135 (1992).
[24] D. Pagel, A. Alvermann, and H. Fehske, Dynamic stark effect, light emission, and entanglement generation in a laser-driven quantum optical system, Phys. Rev. A **95**, 013825 (2017).
[25] T. K. Mavrogordatos, Strong-coupling limit of the driven dissipative light-matter interaction, Phys. Rev. A **100**, 033810 (2019).
[26] H. R. Baghshahi, M. K. Tavassoly, and S. J. Akhtarshenas, Generation and nonclassicality of entangled states via the interaction of two three-level atoms with a quantized cavity field assisted by a driving external classical field, Quant. Inf. Proc. **14**, 1279 (2015).
[27] A. T. Avelar and B. Baseia, Preparing highly excited fock states of a cavity field using driven atoms, J. Opt. B **7**, 198 (2005).
[28] C. C. Gerry, Conditional state generation in a dispersive atom-cavity field interaction with a continuous external pump field, Phys. Rev. A **65**, 063801 (2002).
[29] H. Nha, Y.-T. Chough, W. Jhe, and K. An, Dynamically induced atomic resonance fluorescence and cavity transmission spectra in a driven Jaynes-Cummings system, Phys. Rev. A **63**, 063814 (2001).
[30] C. K. Law and J. H. Eberly, Arbitrary Control of a Quantum Electromagnetic Field, Phys. Rev. Lett. **76**, 1055 (1996).
[31] J. A. Hutchison, T. Schwartz, C. Genet, E. Devaux, and T. W. Ebbesen, Modifying chemical landscapes by coupling to vacuum fields, Angew. Chem., Int. Ed. **51**, 1592 (2012).
[32] R. Balili, V. Hartwell, D. Snoke, L. Pfeiffer, and K. West, Bose-einstein condensation of microcavity polaritons in a trap, Science **316**, 1007 (2007).
[33] J. Schachenmayer, C. Genes, E. Tignone, and G. Pupillo, Cavity-Enhanced Transport of Excitons, Phys. Rev. Lett. **114**, 196403 (2015).
[34] B. Xiang, R. F. Ribeiro, M. Du, L. Chen, Z. Yang, J. Wang, J. Yuen-Zhou, and W. Xiong, Intermolecular vibrational energy transfer enabled by microcavity strong light–matter coupling, Science **368**, 665 (2020).
[35] A. Reserbat-Plantey, I. Epstein, I. Torre, A. T. Costa, P. A. D. Gonçalves, N. A. Mortensen, M. Polini, J. C. W. Song, N. M. R. Peres, and F. H. L. Koppens, Quantum nanophotonics in two-dimensional materials, ACS Photon. **8**, 85 (2021).
[36] D. M. Coles, N. Somaschi, P. Michetti, C. Clark, P. G. Lagoudakis, P. G. Savvidis, and D. G. Lidzey, Polariton-mediated energy transfer between organic dyes in a strongly coupled optical microcavity, Nat. Mater. **13**, 712 (2014).
[37] J. Kasprzak, M. Richard, S. Kundermann, A. Baas, P. Jeambrun, J. M. J. Keeling, F. M. Marchetti, M. H. Szymańska, R. André, J. L. Staehli, V. Savona, P. B. Littlewood, B. Deveaud, and L. S. Dang, Bose–Einstein condensation of exciton polaritons, Nature (London) **443**, 409 (2006).
[38] T. Schwartz, J. A. Hutchison, C. Genet, and T. W. Ebbesen, Reversible Switching of Ultrastrong Light-Molecule Coupling, Phys. Rev. Lett. **106**, 196405 (2011).
[39] J. D. Plumhof, T. Stöferle, L. Mai, U. Scherf, and R. F. Mahrt, Room-temperature Bose–Einstein condensation of cavity exciton–polaritons in a polymer, Nat. Mater. **13**, 247 (2014).
[40] J. A. Hutchison, A. Liscio, T. Schwartz, A. Canaguier-Durand, C. Genet, V. Palermo, P. Samorì, and T. W. Ebbesen, Tuning the work-function via strong coupling, Adv. Mater. **25**, 2481 (2013).
[41] K. Wang, M. Seidel, K. Nagarajan, T. Chervy, C. Genet, and T. Ebbesen, Large optical nonlinearity enhancement under electronic strong coupling, Nat. Commun. **12**, 1486 (2021).
[42] D. N. Basov, A. Asenjo-Garcia, P. J. Schuck, X. Zhu, and A. Rubio, Polariton panorama, Nanophotonics **10**, 549 (2021).
[43] D. Craig and T. Thirunamachandran, *Molecular Quantum Electrodynamics; An Introduction to Radiation Molecule Interactions* (Dover, Mineola, NY, 1984).
[44] M. Ruggenthaler, N. Tancogne-Dejean, J. Flick, H. Appel, and A. Rubio, From a quantum-electrodynamical light–matter description to novel spectroscopies, Nat. Rev. Chem. **2**, 0118 (2018).
[45] V. Rokaj, D. M. Welakuh, M. Ruggenthaler, and A. Rubio, Light–matter interaction in the long-wavelength limit: no ground-state without dipole self-energy, J. Phys. B **51**, 034005 (2018).
[46] A. Mandal, S. Montillo Vega, and P. Huo, Polarized fock states and the dynamical casimir effect in molecular cavity quantum electrodynamics, J. Phys. Chem. Lett. **11**, 9215 (2020).
[47] A. Mandal, T. D. Krauss, and P. Huo, Polariton-mediated electron transfer via cavity quantum electrodynamics, J. Phys. Chem. B **124**, 6321 (2020).
[48] I. V. Tokatly, Conserving approximations in cavity quantum electrodynamics: Implications for density functional theory of electron-photon systems, Phys. Rev. B **98**, 235123 (2018).
[49] D. S. Wang, T. Neuman, J. Flick, and P. Narang, Light–matter interaction of a molecule in a dissipative cavity from first principles, J. Chem. Phys. **154**, 104109 (2021).
[50] J. Flick and P. Narang, Ab initio polaritonic potential-energy surfaces for excited-state nanophotonics and polaritonic chemistry, J. Chem. Phys. **153**, 094116 (2020).
[51] N. Rivera, J. Flick, and P. Narang, Variational Theory of Nonrelativistic Quantum Electrodynamics, Phys. Rev. Lett. **122**, 193603 (2019).
[52] J. Flick, N. Rivera, and P. Narang, Strong light-matter coupling in quantum chemistry and quantum photonics, Nanophotonics **7**, 1479 (2018).
[53] J. Flick and P. Narang, Cavity-Correlated Electron-Nuclear Dynamics from First Principles, Phys. Rev. Lett. **121**, 113002 (2018).
[54] C. Huang, A. Ahrens, M. Beutel, and K. Varga, Two electrons in harmonic confinement coupled to light in a cavity, Phys. Rev. B **104**, 165147 (2021).
[55] J. Malave, Y. S. Aklilu, M. Beutel, C. Huang, and K. Varga, Harmonically confined n-electron systems coupled to light in a cavity, Phys. Rev. B **105**, 115127 (2022).
[56] H. Gao, F. Schlawin, M. Buzzi, A. Cavalleri, and D. Jaksch, Photoinduced Electron Pairing in a Driven Cavity, Phys. Rev. Lett. **125**, 053602 (2020).
[57] V. Rokaj, M. Ruggenthaler, F. G. Eich, and A. Rubio, Free electron gas in cavity quantum electrodynamics, Phys. Rev. Res. **4**, 013012 (2022).

[58] J. Flick, M. Ruggenthaler, H. Appel, and A. Rubio, Kohn–sham approach to quantum electrodynamical density-functional theory: Exact time-dependent effective potentials in real space, Proc. Natl. Acad. Sci. (USA) **112**, 15285 (2015).

[59] J. Keller, G. Scalari, S. Cibella, C. Maissen, F. Appugliese, E. Giovine, R. Leoni, M. Beck, and J. Faist, Few-electron ultrastrong light-matter coupling at 300 ghz with nanogap hybrid lc microcavities, Nano Lett. **17**, 7410 (2017).

[60] M. Halbhuber, J. Mornhinweg, V. Zeller, C. Ciuti, D. Bougeard, R. Huber, and C. Lange, Non-adiabatic stripping of a cavity field from electrons in the deep-strong coupling regime, Nat. Photon. **14**, 675 (2020).

[61] J. Mornhinweg, M. Halbhuber, C. Ciuti, D. Bougeard, R. Huber, and C. Lange, Tailored Subcycle Nonlinearities of Ultrastrong Light-Matter Coupling, Phys. Rev. Lett. **126**, 177404 (2021).

[62] J. Keller, G. Scalari, S. Cibella, F. Appugliese, C. Maissen, E. Giovine, R. Leoni, M. Beck, and J. Faist, Hybrid nano-gap lc-metasurface at 300 ghz ultrastrongly coupled to less than 100 electrons, in *Advanced Photonics 2018 (BGPP, IPR, NP, NOMA, Sensors, Networks, SPPCom, SOF)* (Optica, Zurich, Switzerland, 2018), p. NoM4J.3.

[63] D. M. Welakuh and P. Narang, Tunable nonlinearity and efficient harmonic generation from a strongly coupled light–matter system, ACS Photon. **10**, 383 (2023).

[64] J. Flick, M. Ruggenthaler, H. Appel, and A. Rubio, Atoms and molecules in cavities, from weak to strong coupling in quantum-electrodynamics (qed) chemistry, Proc. Natl. Acad. Sci. (USA) **114**, 3026 (2017).

[65] C. Schäfer, M. Ruggenthaler, and A. Rubio, Ab initio nonrelativistic quantum electrodynamics: Bridging quantum chemistry and quantum optics from weak to strong coupling, Phys. Rev. A **98**, 043801 (2018).

[66] M. Ruggenthaler, J. Flick, C. Pellegrini, H. Appel, I. V. Tokatly, and A. Rubio, Quantum-electrodynamical density-functional theory: Bridging quantum optics and electronic-structure theory, Phys. Rev. A **90**, 012508 (2014).

[67] K. Husimi, Miscellanea in elementary quantum mechanics, II, Prog. Theor. Phys. **9**, 381 (1953).

[68] E. H. Kerner, Note on the forced and damped oscillator in quantum mechanics, Can. J. Phys. **36**, 371 (1958).

[69] J. Crank and P. Nicolson, A practical method for numerical evaluation of solutions of partial differential equations of the heat-conduction type, Math. Proc. Cambridge Philos. Soc. **43**, 50 (1947).

[70] D. Kidd, C. Covington, and K. Varga, Exponential integrators in time-dependent density-functional calculations, Phys. Rev. E **96**, 063307 (2017).

[71] M. Uemoto, Y. Kuwabara, S. A. Sato, and K. Yabana, Nonlinear polarization evolution using time-dependent density functional theory, J. Chem. Phys. **150**, 094101 (2019).

[72] V. A. Goncharov and K. Varga, Real-space, real-time calculation of dynamic hyperpolarizabilities, J. Chem. Phys. **137**, 094111 (2012).

[73] Y. Suzuki, M. Suzuki, and K. Varga, *Stochastic Variational Approach to Quantum-mechanical Few-body Problems* (Springer Science & Business Media, Berlin, Heidelberg, 1998), Vol. 54.